Journal of Contaminant Hydrology 106 (2009) 150–165

Contents lists available at ScienceDirect

Journal of Contaminant Hydrology

journal homepage: www.elsevier.com/locate/jconhyd

The effects of scale and spatial heterogeneities on diffusion in volcanic breccias and basalts: Amchitka Island, Alaska

Jennifer L. Benning *, David L. Barnes

Department of Civil and Environmental Engineering, Water and Environmental Research Center, University of Alaska Fairbanks, 306 Tanana Drive, Duckering Building. Rm 245, Fairbanks, Alaska 99775-5900, USA

ARTICLE INFO

Article history:
Received 6 October 2008
Received in revised form 6 February 2009
Accepted 8 February 2009
Available online 21 February 2009

Keywords:
Diffusion coefficient
Formation factor
Scale effects
Heterogeneities
Probability density function

ABSTRACT

Knowledge of the factors that influence the diffusion of contaminants, such as the diffusivity and the connected porosity, is crucial to modeling the long-term fate and transport of contaminants in subsurface systems with small or negligible advective flow, such as in fractured crystalline rock. Fractured rock is naturally heterogeneous, and hence, understanding the diffusivity of a molecule through this material (or the formation factor of the medium) becomes a complex problem, with critical concerns about the scale of laboratory measurements and about the spatial variability of these measurements relative to the scale needed for fate and transport modeling. This study employed both electrical and tracer-based laboratory methods to investigate the effects of scale and pore system connectivity on the diffusivity for volcanic matrix rock derived from the study site, a former underground nuclear test site at Amchitka Island, Alaska. The results of these investigations indicate a relatively well-connected pore system with scale effects generally limited to approximately 6 cm lengths and well-correlated to observed heterogeneous features. An important conclusion resulting from this study, however, is that there is a potential for the estimated diffusivity to be misrepresented by an order of magnitude if multiple samples or longer sample lengths are not used. Given the relatively large number of measurements resulting from these investigations, an analysis of the probability density function (PDF) of the diffusivity was possible. The PDF of the diffusivity was shown to generally follow a normal distribution for individual geologic layers. However, when all of the geologic layers are considered together, the distribution of the subsurface as a whole was shown to follow a lognormal distribution due to the order of magnitude differences amongst the layers. An understanding of these distributions is essential for future stochastic modeling efforts.

1. Introduction

When the advective flow in the subsurface is small or negligible, the diffusion of contaminants can play a dominant role in their transport. This is often the case when the subsurface is comprised of fractured crystalline rock (Neretnieks, 1980, 1993). Several comprehensive studies on diffusive transport have been conducted in this geologic material owing to the choice of this media for nuclear waste repositories and as the host media for several historic underground nuclear tests (Bradbury and Green, 1985; Skagius and Neretnieks, 1986a; Reimus et al., 2007). Others have established that the knowledge of the factors that influence the diffusion of contaminants, such as the diffusivity (or formation factor, the ratio of the intrinsic diffusion coefficient to the molecular diffusion coefficient) and the connected (or effective) porosity, is crucial to modeling the long-term fate and transport of contaminants in these systems (Bradbury and Green, 1985; Skagius and Neretnieks, 1986a; Löfgren and Neretnieks, 2006; Appelo and

* Corresponding author. Tel.: +1 907 474 5396; fax: +1 907 474 6087.
E-mail addresses: fnjlb2@uaf.edu (J.L. Benning), ffdlb@uaf.edu (D.L. Barnes).

0169-7722/$ – see front matter © 2009 Elsevier B.V. All rights reserved.
doi:10.1016/j.jconhyd.2009.02.005

Wersin, 2007). However, accurate measurement of these factors, primarily formation factor, is difficult due to the spatial heterogeneity of these properties and the possible scale dependency of these measurements.

The objectives of this study were to investigate the effects of scale and pore system connectivity on the intrinsic diffusion coefficient for volcanic matrix rock and to investigate the impacts of spatial heterogeneities, particularly in regards to highly heterogeneous breccias, on intrinsic diffusion coefficients. In order to contribute to possible future stochastic modeling efforts in groundwater flow and contaminant transport, an associated objective of this study was to analyze the probability density function (PDF) of the diffusivity (or formation factor). Because the PDF of the formation factor is strongly tied to the porosity, a comparison of the formation factor/porosity relationships from this study were compared to the relationships in published literature. For the study site, Amchitka Island, a former underground nuclear test site, a previous groundwater and contaminant transport model indicated that the porosity and the intrinsic diffusion coefficient are two of the key uncertainties (Hassan et al., 2002). Thus, an associated objective of this study was to assess the range of diffusivities found in the different rock types that comprise the subsurface of the island. Recommendations for radionuclide transport modeling at Amchitka Island are made in light of these effects. This study employed both electrical and tracer-based laboratory methods to investigate the effects of scale and pore system connectivity on the diffusivity for volcanic matrix rock derived from the study site, a former underground nuclear test site at Amchitka Island, Alaska. Significantly more data are derived from the electrical methods, however, the application of tracer-based methods allows a comparison of the methods used to derive the diffusion parameters.

2. Background

2.1. The effects of scale and spatial heterogeneities on diffusion

Fractured rock is naturally heterogeneous, and hence, understanding the diffusivity of a molecule through this material becomes a complex problem, with critical concerns about the scale of laboratory measurements relative to the field scale and about the spatial variability of these measurements relative to the scale needed for fate and transport modeling. Numerous studies have indicated the influence of scale on such parameters as porosity (Bear, 1972) and longitudinal dispersivity (Gelhar et al., 1992), and it logically follows that there may be similar effects of scale on diffusion, particularly in fractured rock. The potential impacts of this inference are particularly a concern with diffusion in fractured rock, as the properties of the media can be very heterogeneous over small scales. Additionally, because the diffusion process is inherently very slow, small samples are typically chosen for laboratory studies, making it difficult to represent the degree of heterogeneity present in the rock. Lever et al. (1985) suggested a minimum thickness for through-diffusion studies on granites of 5 mm due to the interconnectivity of pores at lesser thicknesses that would otherwise be unconnected at greater lengths. However, this minimum thickness depends on the nature of the rock, and one would anticipate that it may be different for different materials.

Atkinson and Titchell (1985) and Skagius (1986) investigated the effects of scale on laboratory-scale diffusion measurements via electrical resistivity methods. Atkinson and Titchell compared the derived formation factors for an Altnabreac granite sample and a Cornish granite sample at decreasing sample lengths, down to 1 cm. The results indicate that the Altnabreac granite, which is characterized by smaller microstructural scale than the Cornish granite, displayed an increase of a factor of 2 in the formation factor at lengths below 5 cm, with no additional changes from 5 cm to 25 cm. However, in the Cornish granite, there was considerably greater scatter in the measured formation factor as a function of diffusion length, presumably due to the greater heterogeneity of that rock. Skagius found that for Swedish crystalline rocks, the formation factor at 5 cm was approximately half the formation factor at 1 cm, with no further scale effects observed between 5 cm and 30 cm.

Valkiainen et al. (1996) studied the effects of sample length on the derived intrinsic diffusion coefficients (as defined by Bradbury and Green, 1985) from through-diffusion experiments on samples of 2, 4, and 6 cm thicknesses. For the Finnish granites studied, their results indicated that, though there was some decrease in pore connectivity and diffusion coefficients between 2 and 4 cm, this decrease was minimal. Löfgren and Neretnieks (2006) investigated the effects of the sample length on the diffusivity for granites and mafic vulcanites using through-diffusion tests, electrical resistivity (AC and DC) experiments, and through-electromigration (TEM) tests. Their results indicated that there were no discernable effects of scale, as the variability between samples was greater than any effects of scale, thus indicating that for the studied rocks, the pore system was well-connected.

Numerous studies have been conducted to assess the spatial heterogeneity of the diffusion of molecules through fractured rock. These studies have focused on various scales of investigations, from inter-site comparisons (Reimus et al., 2007), to comparisons across a site (Bradbury and Green, 1985; Skagius and Neretnieks, 1986a,b; Yamaguchi and Nakayama, 1998), and to studies into the effects of microscopic heterogeneities (Siitari-Kauppi et al., 1997; Tidwell et al., 2000; Altman et al., 2004).

On the laboratory scale, the influences of heterogeneous porosity on diffusion coefficients have been investigated by Siitari-Kauppi et al. (1997), Tidwell et al. (2000), and Altman et al. (2004). Siitari-Kauppi et al. (1997) examined heterogeneities of mica gneiss samples and tonalite samples with varying degrees of alteration. Tidwell et al. (2000) and Altman et al. (2004) used X-ray absorption imaging to examine the relationship between heterogeneities in porosity and diffusion at the sub-millimeter scale in Culebra dolomite samples from New Mexico and fractured granodiorite samples from Japan. In both studies, spatial variabilities in diffusion coefficients were well-correlated with heterogeneities in void space features.

It has been demonstrated that the degree of connectivity of the pore structure plays an important role in the movement of molecules by diffusion in fractured rock, though different investigations have lead to different conclusions regarding the extent of the pore connectivity (Löfgren and Neretnieks, 2006). Schild et al. (2001) conducted *in situ* testing of connected porosity in granitic matrix rocks with porosities

less than 1% using acrylic impregnation methods. Their study found that the rocks displayed a well-connected system of microcracks. These results were somewhat in contradiction of an earlier, more qualitative study by Heath et al. (1992), who found that the extent of connectivity was limited. This study investigated spatial variability of diffusion by examining changes in microstructure, physical properties, and geochemical properties of rock at increasing distances from fractures in samples representing El Berrocal granites in Spain, Stripa granite in Sweden, and Whiteshell granite in Canada. The study's results indicated that all of the samples display a "zone of enhanced mobility" surrounding the fracture, which extends from 25 mm to 80 mm, depending on the rock type and degree of alteration. The authors concluded that in undisturbed rock, not all of the media may be available for retardation via diffusion, as many models assume. Later investigations into the connectivity of the pore system in Swedish granites by Löfgren and Neretnieks (2006) concluded that the pore systems were well-connected at a scale of meters. It is noted, however, that most of these studies focused on the connectivity of intrusive igneous rocks, and that for other types of matrix rocks, the conclusions could be different.

2.2. Probability density function of formation factor

In stochastic models of groundwater flow and contaminant transport, knowledge of the forms of the probability distributions for various parameters is essential. Despite its potential importance to modeling efforts, the forms of the probability density functions of the diffusion coefficient and formation factor are not well established in current literature. Theoretically, the intrinsic diffusion coefficient should have the same form of the probability density function (PDF) as the formation factor and should depend on the combined effects of the porosity and the pore structure properties, tortuosity and constrictivity. It is probable that the distribution of the formation factor could, in part, be explained by the nature and distribution of the pore structure. Towle (1962) notes that the distributions of the pore sizes of rocks are unknown, but that they should be "strongly tied" to the particle size distribution. Lin et al. (1986) found that pores are "usually anisotropic, unevenly distributed and strongly heterogeneous with the formation, and have a skewed logarithmic size distribution."

In an analysis of concrete structures for nuclear containment, Snyder (2003) indicates that the expected distribution of the formation factor for concrete is unknown, though it is likely either normal or lognormal. Löfgren (2007) analyzed the probability density functions for two boreholes at a site in Forsmark, Sweden using the results of extensive in situ electrical resistivity logging. The results of this study, conducted at a site comprised generally of intrusive igneous matrix rock, indicated that the formation factor in both wells corresponded "fairly well" with a log-normal distribution. It is unknown if this form of the PDF of the formation factor would be similar at other sites comprised of a different type of subsurface matrix.

2.3. Amchitka Island

Amchitka Island is one of the western Aleutian Islands and is part of a group of islands known as the Rat Islands (Fig. 1). Three underground nuclear tests were conducted on Amchitka between 1965 and 1971. The first test, Long Shot, was an 80-kt (kiloton TNT equivalent) nuclear explosion detonated on 29 October 1965 at a depth of 701 m (2300 ft) below ground surface. The 1-Mt (megaton TNT equivalent) nuclear device, named Milrow, was detonated on 2 October 1969 at a depth of 1218 m (3996 ft) below ground surface. The final explosion, Cannikin, at approximately 5-Mt, was the largest nuclear device ever detonated in the US underground testing program and was detonated on 6 November 1971 at a depth of 1792 m (5643 ft) (USAEC, 1972; Claassen, 1978; Merritt and Fuller, 1977; US Congress, 1989).

As part of a process undertaken by the U.S. Department of Energy to assess the human health risk resulting from the possible release of radionuclides to the marine environment as a consequence of the tests, Hassan et al. (2002) produced a model to describe Amchitka Island's groundwater flow and the transport of radionuclides released during the three tests. This modeling effort also included sensitivity analyses in order to ascertain the relative significance of the many uncertainties in the model. The analyses revealed that two of the key uncertainties are the

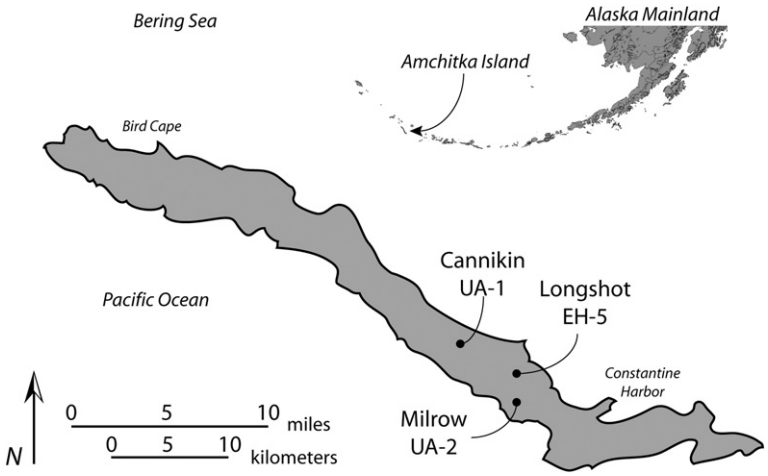

Fig. 1. Map of Amchitka Island, Alaska, showing the locations of the three underground nuclear tests, Long Shot, Milrow, and Cannikin.

porosity and the intrinsic diffusion coefficient, indicating the importance of accurately representing the intrinsic diffusion in fractured rock contaminant transport modeling. Later groundwater and transport models for the island, summarized in Benning et al. (2009), based on additional data reduced some of the uncertainties associated with the island's earlier models; however, as noted by Pletnikoff (2008) and Benning et al. (2009), there are still remaining concerns regarding the uncertainties, namely the porosity and retardation through diffusion, associated with the modeling efforts at the site.

The intrinsic diffusion coefficients at Amchitka Island have been investigated in basalts and breccias by Brown (2000) and in an andesite sample by Raghupatruni (2004). Brown found intrinsic diffusion coefficients for bromide from small samples (with maximum sizes of $3.8\times1.9\times1.9$ cm and $2\times2\times0.5$ cm) of 5.9×10^{-11} and 6.8×10^{-10} m^2/s for basalt samples and 1.2×10^{-11} and 2.6×10^{-11} m^2/s for the breccia samples. In that study, it was noted that the variability of the breccia diffusion coefficients for different samples was greater than for different basalt samples, and this is likely due to the more heterogeneous nature of breccia, particularly at the scale of the samples used. The origin of the core samples used in this study was given as in the vicinity of the Cannikin test shot, though no information was given as to the depth from which the samples were obtained. Raghupatruni (2004) found intrinsic diffusion coefficients of 6×10^{-12} and 2×10^{-10} from adjacent samples of andesite core, originating from a core in the vicinity of the Milrow test shot, with no information given on the depth from which the sample was obtained. The higher value is in the same order of magnitude as the molecular diffusion coefficient, indicating the likelihood that a microporous preferential pathway existed in the sample. The order of magnitude differences between the two andesite samples and the two-order of magnitude differences between the andesite diffusivities and those of the basalts and breccias indicate that the spatial variability of diffusivities at the island warranted further investigations.

Table 1
Location and lithologic description of the drill core sections sampled from the UAe-1 drill hole analyzed in this study, from Gard et al. (1969a,b).

Core	Depth below grade (m)	Lithologic description
4	456–459	Basalt, dark gray, dense, massive. Contains small feldspar and pyroxene phenocrysts. Core shows discontinuous fractures well healed with chalcedony.
7	734–737	Breccia, greenish-black, dense, devitrified. Matrix contains basalt fragments, a few purple andesite fragments as large as 7.5 cm, a few green chloritized rock fragments, and some pyrite and pyroxene crystals as large as 5 mm. Average fragments size 5 mm.
8	768–781	Breccia, black, slightly devitrified, very dense and brittle. Devitrified greenish-black matrix contains resinous vitric spherulites and feldspar laths. Black vesicular glass fragments average 2.5 cm and contain radially fibrous zeolites in vesicles. Core contains one rectangular fragment of fine-grained light-gray diorite.
15	1155–1158	Breccia, black, devitrified. Fragments devitrified, average size 5 mm. One large (20 in.) basalt fragment in core is medium-gray, very fine grained. Basalt has vesicles filled with zeolites and displays chilled margin.
16	1228–1236	Basalt, aphanitic to fine-grained, porphyritic with phenocrysts of pyroxene (augite). Felted groundmass of plagioclase and glass.
19	1412–1414	Breccia, greenish-black, very dense, brittle, altered. Matrix contains small (<12 mm) aphanitic basalt fragments. Zeolites and chalcedony distributed throughout; some pyroxene crystals in matrix.
20	1501–1503	Breccia, greenish-gray, soft, devitrified, argillized. Zeolites and chalcedony throughout. Fragments are argillized glass and basalt. Pyroxene crystals in matrix.
24	1593–1596	Breccia, mottled pale-green and very light gray, propylitized. Lithic fragments range in size from 1 mm to 1 cm and are subrounded to rounded, predominantly basalt. Fine-grained clayey matrix, constitutes about 10% the rock and contains rare pyroxene crystals.
36	1710–1730	Interbedded sandstone and fine-grained breccia. Composed of volcanic rock fragments, minute augite grains, and opaque minerals. Whole rock is propylitized.

3. Materials and methods

3.1. Samples

The investigations focused on core samples from Amchitka Island, Alaska, at the UAe-1 drill hole, which is in the immediate vicinity of the Cannikin underground nuclear test shot. The drill hole was advanced in 1965 as an exploratory core prior to the nuclear detonations. Drill core sections used in these investigations are limited to the remaining sections of core that are still intact due to the high costs and health risks associated with obtaining post testing core samples from Amchitka Island. A list of the drill core sections tested in these studies, including the lithologic descriptions and core section depths, is included in Table 1. For Cores 7, 8, and 24, multiple samples were tested from the same lithologic layer, or drill core section; these samples are denoted as #1, #2, etc., throughout this paper. Similarly, when multiple experimental methods (i.e. electrical and tracer-based methods on Core 19 and Core 24 drill core section samples), approximately adjacent samples were cut from the same drill core section and used in the various experiments. Preliminary electrical conductivity investigations were conducted on two samples, an andesite derived from the UAe-2 drill hole, in the immediate vicinity of the Milrow test shot, and a porous breccia (Core 87) derived from the UA-1 drill hole, in the Cannikin test shot vicinity. Due to weathering of the core sample boxes, the sample depth from the UAe-2 core sample was not identifiable. However the results of the two samples are included because they represent the highest and lowest estimated rock diffusivities at the site. All of the drill core sections investigated were 89 mm (3.5 in.) in diameter. Prior to conducting other investigations, the bulk porosity of each cut sample was measured via the water saturation method (Fetter, 1994), in which all samples were oven-dried until a stable mass was achieved and then saturated under vacuum pressure. The densities of the saturating fluid, discussed in the following, were measured and applied to the porosity calculation.

3.2. Experimental

3.2.1. Through-diffusion

In a typical through-diffusion experiment, several parameters, including the intrinsic diffusion coefficient, the

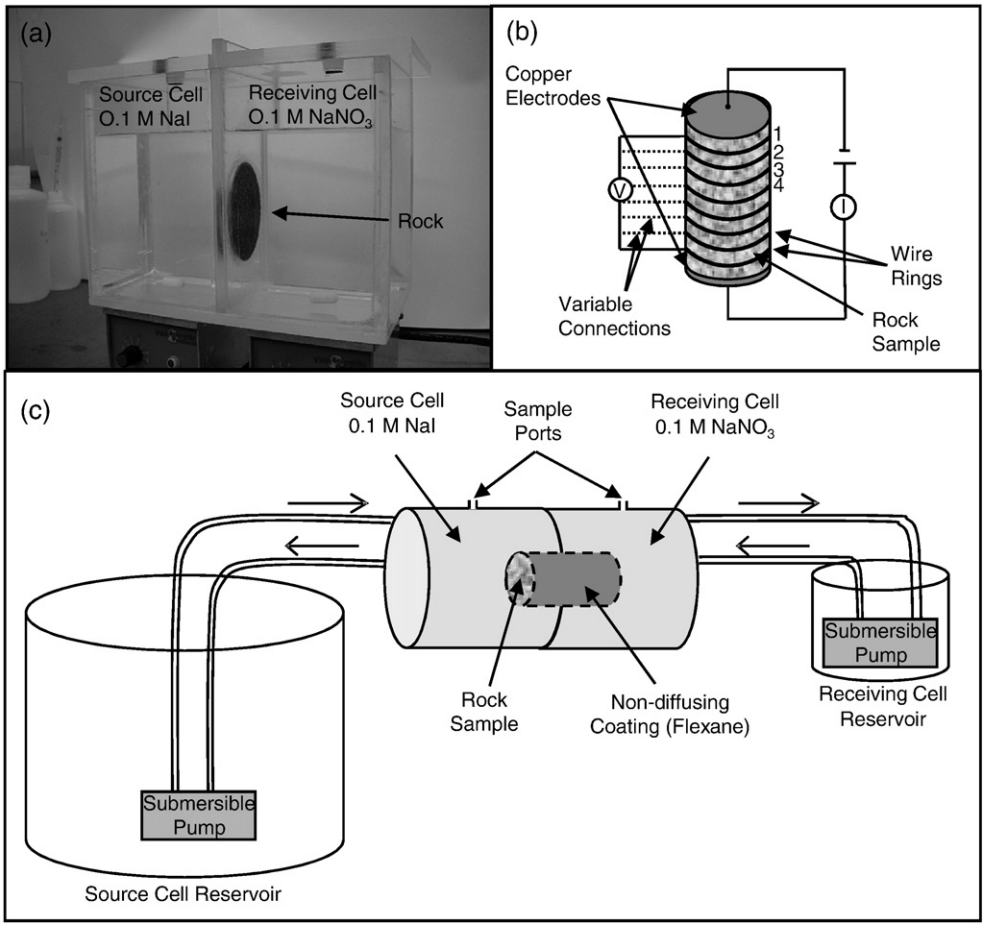

Fig. 2. Illustrations of experimental apparatus for: (a) through-diffusion (b) electrical conductivity (c) modified through-diffusion.

formation factor, and the effective porosity, are derived from the application of Fick's Law of diffusion to the experimental data. In the ensuing discussion, it is important to clarify the definitions of these parameters, since they are defined differently by many researchers. Bradbury and Green (1985) provide thorough review of the different diffusion coefficients used for porous media, and therefore, in the ensuing discussions, the coefficients used are consistent with their terminology. In this study, the intrinsic diffusion coefficient, D_i, is defined as (Van Brakel and Heertjes, 1974):

$$D_i = D_m\left(\frac{\phi_e \delta}{\tau^2}\right) = D_p\phi_e = D_m F_f = G_f{*}\theta{*}D_m\frac{G_f}{\phi_e}D_m \qquad (1)$$

where D_m is the free water or molecular diffusion coefficient, D_p is the pore water diffusion coefficient, ϕ_e is the effective or transport porosity, δ is the constrictivity, and τ is the tortuosity of the porous medium. F_f is the formation factor and is considered to be solely a property of the porous medium and not a property of diffusing molecule; however, as noted by Snyder (2001), it can reflect the specific conditions of the experiment. The geometric factor, G_f, of a porous medium is used to describe the structure of the pore network.

Several through-diffusion (TD) experiments, using iodide as a conservative tracer, were conducted as described in literature (Bradbury and Green, 1985; Skagius and Neretnieks, 1986a,b; Snyder, 2001). The first set of TD experiments were conducted on relatively thin slices of drill core sections in an appropriately designed TD experimental apparatus (TD I). These experiments were conducted on two breccia samples derived from Cores 19 and 24. The Core 19 and Core 24 samples were cut using a diamond saw to thicknesses of 5.2 mm and 7.7 mm, respectively. The dry samples were affixed to an acrylic plate using Lexel® caulk. The plate was then affixed into an acrylic box, shown in Fig. 2a. The receiving cell was filled with 0.1 M sodium nitrate ($NaNO_3$) and allowed ample time to achieve rock saturation, based on conservative estimates using the measured permeability of each sample. The source cell was then filled with a conservative tracer solution, 0.1 M sodium iodide (NaI), with the solution volume adjusted to achieve equal hydrostatic pressures on either side of the rock sample. Throughout the experimental duration, 5 mL samples were collected from both the source and receiving cells, and after the sample event, 5 mL of 0.1 M NaI and 0.1 M $NaNO_3$ were replaced in the source and receiving cells, respectively. The experiments were conducted at constant temperatures of 21 ± 1 °C and 23 ± 0.5 °C for the Core 19 and Core 24 experiments, respectively. Each cell was kept mixed throughout the experimental duration through the use of magnetic stir bars. The experimental design and

uncertainty analyses are discussed in more thorough detail in Benning (2008).

A second configuration of the through-diffusion experimental apparatus (TD II) was also employed in these studies in order to test samples of breccias that are thicker than the size of clasts present in the breccia drill core sections. In order to examine the potential effects of scale, this second through-diffusion experimental reactor (TD II) was designed to accommodate samples thicker than the size of the clasts present in the breccia samples. This test was conducted on 5.6 cm sample cut from the Core 24 breccia drill core section. In preparation for the test, the sample was first washed in deionized water and then oven-dried. The sample was then placed in a fabricated mold and coated around the circumference via injection of Flexane® polyurethane. The two ends were left uncoated so that diffusion of a tracer can occur only along the axial direction. The molded coating includes a ridge which acts as an O-ring to seal the two ends of the diffusion reactor. The aluminum reactor cell (see Fig. 2c), with the coated rock in between was compressed and bolted together, with the rock dividing the source and measurement cells. The receiving cell was filled with a 0.1 M $NaNO_3$ solution, connected with tubing to a secondary receiving solution reservoir. The rock sample was saturated with this solution under vacuum pressure.

Once saturation had been achieved, the source cell was filled with a 0.1 M NaI tracer solution. Both the source cell and receiving cells were connected to secondary reservoirs, such that the total cell volumes were approximately 18 L and 2.4 L for the source and receiving cells, respectively. The use of the secondary reservoirs enabled mechanical mixing so that samples would be representative of the entire cell volumes. For the source cells, the use of a large volume secondary reservoir was used to approximate a constant and relatively high source cell concentration condition in comparison to the receiving cell concentration. Both the source and receiving cells were kept mixed by circulating fluid at low flows using submersible pumps in the respective source and receiving cell secondary reservoirs. The pumps were set on timers in order to minimize heating. The experiments were conducted at constant temperatures of 23 ± 0.5 °C.

The Core 24 sample reactor source pump failed after approximately 1 year, causing a change in the early-time boundary conditions for the experiment. After a new pump was installed, steady-state conditions were achieved, allowing the use of the time-lag solution (as discussed in the following) to determine the intrinsic diffusion coefficient of this sample. The source cell concentration was constant, within experimental error, during this time period. This equipment failure prohibited the use of the semi-analytical solution to Fick's Law and the intrinsic diffusion coefficient had to be calculated using the time-lag solution. The lack of transient-state data prevented the determination of the effective porosity for this sample. A through-diffusion experiment was also attempted on a 4.9 cm sample from Core 19; however, due to equipment failure no diffusion data could be obtained.

There are numerous solutions for Fick's Law of diffusion to determine the intrinsic diffusion coefficient and effective porosity from through-diffusion experimental data. Some of these solutions and their assumed boundary conditions are summarized and compared in Benning (2008). The two methods employed in these investigations are the time-lag method (Crank, 1975; Bradbury and Green, 1985; Skagius and Neretnieks, 1986a,b) and the semi-analytical method (Moridis, 1998, 1999). For typical through-diffusion experiments conducted on relatively thin core samples, the semi-analytical method was used to derive the intrinsic diffusion coefficients and effective porosities. The semi-analytical solution provides a more reliable estimate of the effective porosity than the time-lag solution when there is sufficient transient-state data for analysis (Benning, 2008).

As indicated in Eq. (1), the formation factor for each sample is calculated by dividing the intrinsic diffusion coefficient by the molecular diffusion coefficient for iodide. The molecular diffusion coefficient of iodide at 25 °C is 2.048×10^{-9} m^2/s at 25 °C (CRC, 2008). This value was adjusted for the correct temperature for each experiment using the Wilke and Change Equation (Treybal, 1980) with published parameters (CRC, 2008). In the experiments, the receiving cell contained an electrolyte solution at 0.1 M concentration, which could introduce some error due to counter-diffusion and electrochemical effects (Krishna and Wesselingh, 1997). However, studies by Stokes et al. (1957), Cussler (1984), Daniel and Albright (1991), and Snyder (2001) indicate that at the molarities used in these experiments, the decrease in the molecular diffusion coefficient is less than 10%.

3.2.2. Chemical analyses

Iodide concentrations were measured by ion chromatography, using a Dionex AS40 Autosampler with an AS-11 Analytical Column and an AG-11 Guard Column and sodium bicarbonate as an eluent. The analytical error was assessed to be a maximum of 6%, and the method detection limit was 2 mg/L for all but the Core 24 TD I test, which had a detection limit of 0.5 mg/L as a result of analytical method modifications. The analytical methods, instrument and measurement errors, and uncertainty analyses are discussed in detail in Benning (2008).

3.2.3. Electrical conductivity

Electrical conductivity testing has commonly been applied to measure formation factors in rock samples (Keller and Ibrahim, 1982; Atkinson and Titchell, 1985; Skagius and Neretnieks, 1986b; Snyder, 2001; Löfgren and Neretnieks, 2006; Mayr et al., 2007). In this method, core samples are saturated with an electrolyte solution at concentrations high enough to overcome potential surface conductivity effects, and then the conductivity of the saturated core is measured (Brace et al., 1965; Skagius and Neretnieks, 1986b; Snyder, 2001). The conductance of the saturated sample will be caused almost exclusively by the solution filling the pore spaces if the rock minerals are nonconducting, and thus depends on the same factors as does the effective diffusion (Klinkenberg, 1951). The Nerst–Einstein Equation relates the conductivity of a solution (κ_S) to its molecular diffusion coefficient (Löfgren and Neretnieks, 2002):

$$\kappa_S = \frac{F^2}{RT} \sum z_i C_{p,i} D_{m,i} \tag{2}$$

When considering the conductivity of a porous medium saturated with an electrolyte solution (κ_R), in the absence of

sorption or surface conduction, the equation is modified by the formation factor:

$$\kappa_R = \frac{F^2}{RT} F_f \sum z_i C_{p,i} D_{m,i} \quad (3)$$

Combining Eqs. (2) and (3) gives:

$$F_f = \left(\frac{D_e}{D_m}\right) = \left(\frac{\kappa_R}{\kappa_S}\right) \quad (4)$$

where the conductivity of the brine-saturated rock is determined by measuring the potential drop (ΔU) and current (i) across electrodes and is calculated from the relationship:

$$\kappa_R = \frac{IL}{\Delta UA} \quad (5)$$

The core samples were oven-dried, then saturated with a 1 M sodium chloride (NaCl) solution under vacuum pressures over a period of four weeks to six months, depending on the size and porosity of the sample. Once saturated, the samples were wrapped in a test sleeve held in place with compression fittings. The test sleeve was constructed of neoprene, with a series of electrodes (rings of copper wire) affixed at 1 cm separations (except for the Core 24 #1 sample test, which used 2 cm separations) equidistantly along the length of the sleeve (along the axial direction on the corresponding core sample). Copper plate electrodes were attached to each end of the core and a conductive gel was used between the rock and plate to ensure contact. A direct current was passed through the sample with a system potential of 3 V and a system current of approximately 1 mA. The experimental system is illustrated in Fig. 2b. Preliminary electrical conductivity tests were conducted without the use of the series of copper wire rings, according to the methods described in Telford et al. (1990), on the UAe-2 andesite and Core 87 breccia samples.

The electrical potential across pairs of adjacent electrodes (i.e. across electrodes 1 and 2, 2 and 3, 3 and 4, etc. to the last electrode, as determined by the sample length summarized in Table 3, as indicated in Fig. 2(b)) was measured across the length of the drill core sample, approximating 1-cm thick, adjacent subsamples, in order to estimate the effects of spatial heterogeneities on diffusion coefficients. For investigations into the effects of scale, the electrical potential was measured across pairs of electrodes spaced at increasing length intervals (i.e. from a 1 cm length, to 2 cm length, etc.). This was accomplished by measuring the potential across electrodes 1 and 2, 1 and 3, 1 and 4, etc. to the last electrode determined by the sample length summarized in Table 3, as illustrated in Fig. 2(b). Since the current across the circuit changed with time, it was simultaneously measured and recorded with the potential readings for use in Eq. (5); the maximum decrease in the current for the experiments was 13%, but typically was less than 5%. The brine solution conductivity was measured for each experiment using a standard conductivity probe and meter, and this measurement was applied in Eq. (4) to determine the sample formation factor.

It is recognized that there are several possible sources of error in the electrical conducting experimental method, such as: the potential for gaps between the electrodes and rock sample; the buildup of pH in the conductive gel and rock sample; and the potential for pacified electrodes. Though no formal uncertainty analysis was performed on these experiments, a series of tests were conducted to determine the effects of the use of DC on the results. In the first test (on the Core 24 #1 breccia sample), an adjustable DC power source was used for the system, set at a system potential of 12 V and a system current of approximately 0.02 A. In these tests, there was an 18% decrease in the system current, indicating possible issues resulting from the pacification of electrodes. Based on this, all subsequent experiments were performed using with the power source set at system potential of 3 V and a system current of approximately 1 mA to reduce these effects. The decrease in current over the course of the experiment was lower under these conditions. As a secondary check, a conventional resistivity sounding meter (OYO Co., Ltd., McOHM model-2115) was used on the same core sample. The meter alternates direct current with a square wave function at a frequency of a few hertz to eliminate the buildup of pH on the electrodes. The results from this test were within 30% of the results obtained with DC current with relatively low voltage and current. As a tertiary check to the potential influences pH buildup, the experiments were all immediately repeated and several of the experiments were repeated with the system polarity reversed. The experimental error from repeat experiments and reverse polarity experiments were a maximum of 12% and 9%, respectively, though generally, the errors were less than 5% in both cases. Löfgren and Neretnieks (2006) performed comparisons of formation factors derived from AC methods and DC methods. In their experiments, the authors eliminated the effects of pH buildup in the DC methods through the use of a secondary electrolyte reservoir on both the cathode and anode sides of the circuit. The differences between the formation factors derived by the AC and DC methods in that study were approximately 10% at maximum.

4. Results and discussion

4.1. The effects of scale on diffusion

The through-diffusion experimental results and the subsequent derivation of the intrinsic diffusion coefficients and effective porosities are presented in Benning (2008). The uncertainty analyses associated with these methods are also discussed in Benning (2008). The intrinsic diffusion coefficients, measured bulk porosities, effective porosities (where applicable), and formation factors for the tests conducted on samples from the Core 19 and Core 24 drill core sections are summarized in Table 2, along with the associated sample length and method of measurement for each value.

The formation factor derived through the electrical conductivity testing for the Core 19 sample is a factor of 1.6 to 5.0 greater than the formation factor derived by the through-diffusion experiment on an approximately adjacent sample. This discrepancy is consistent with the results of others, such as Ohlsson (2000) and Löfgren and Neretnieks (2006), who found that formation factors derived by electrical methods were higher than those derived from tracer based methods by approximately a factor of 2 for the Swedish granites studied. Walter (1982) reported similar results for volcanic tuff samples. Several authors propose that the conductivity of the rock minerals (Keller and Ibrahim, 1982) and anion exclusion (Löfgren and Neretnieks, 2006) in the tracer-based methods are potential causes for these differences.

Table 2
Comparison of formation factors and porosities derived from different sample lengths and different methods for approximately adjacent breccia samples derived from the noted drill core sections.

Sample	Length (cm)	Porosity (%)	Method	Formation Factor	Method
Core19	0.5	13.7	Water balance	7.4×10^{-4}	Through-diffusion I
		6.0	Through-diffusion		
	33	13.4	Water balance	1.2×10^{-3}–3.7×10^{-3}*	Electrical conductivity
				2.8×10^{-3} (average)	
Core 24	0.8	16.8	Water balance	6.4×10^{-3}	Through-diffusion I
		15.0	Through-diffusion		
	5.6	16.7	Water balance	4.4×10^{-3}	Through-diffusion II
	28	19.0	Water balance	9.2×10^{-3}–1.2×10^{-2}*	Electrical conductivity
				1.1×10^{-2} (average)	
	33	16.3	Water balance	4.1×10^{-3}–8.9×10^{-3}*	Electrical conductivity
				6.1×10^{-3} (average)	

* Note: The ranges given are for the formation factors derived from the adjacent 1-cm subsamples for each sample.

The formation factor of the first Core 24 sample tested using electrical methods is a factor of 1.4 to 1.9 greater than that derived by the through-diffusion experiment and a factor of 2.1 to 2.7 greater than that derived by the second through-diffusion experiment (Table 2) for that sample from the drill core section. However, the measured porosity of that sample (Core 24 #1), 19.0%, is also greater than the measured porosities, 16.3 to 16.8%, of the samples tested with the TD I and TD II experiments. In comparison, the formation factors derived by the TD I and TD II methods both fall within the range of those estimated by electrical methods on a similar porosity sample (Core 24 #2), indicating that: the mineral content of this sample is not influencing the formation factor derived by electrical methods, anion exclusion in the tracer methods is negligible, and/or there is less variability between samples from this drill core section than from the Core 19 drill core section.

However, even with these noted differences between the derived formation factors for the various drill core samples using the different methods, overall, the formation factors derived using different methods are relatively close and, as will be discussed in Section 4.2, are typically less than the sample to sample variability. This indicates comparability between electrical and tracer-based methods.

The formation factors derived from increasing sample axial lengths in the electrical conductivity experiments for all of the samples indicated in Table 1 are illustrated as a function of experimental length in Fig. 3. Fourteen samples were tested from nine different drill core sections. In most of the samples, there is some variability in formation factor with increasing sample length, but then at some length, the formation factor approaches an approximately asymptotic value, indicating no additional scale dependency. This length is different for each sample and, as will be discussed in the subsequent, depends on the degree of heterogeneity in the sample. The approximate asymptotic formation factor value, chosen as less than +/− 10% variation, and the approximate length required to achieve that value for each sample are

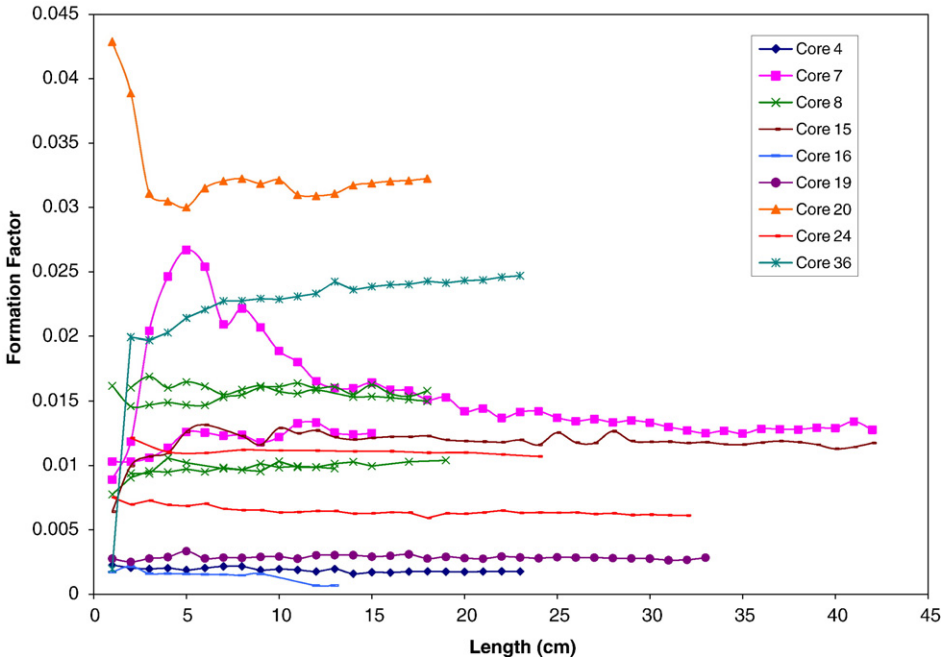

Fig. 3. The influence of sample length on the formation factor measured by electrical conductivity testing.

Table 3
The maximum, minimum, and average formation factors derived from electrical conductivity testing on adjacent axial sections of core samples (with the factor as the ratio of the maximum to minimum formation factor); the asymptotic values of the formation factor, defined here by variations of less than +/− 10%, and the lengths required to achieve the asymptotic value.

Sample	Length (cm)	Porosity	Formation factor × 10^2					
			Minimum	Maximum	Factor (max/min)	Average	Asymptotic	Length to asymptote (cm)
UAe-2 andesite	2	0.093	–	–	–	0.013	–	–
Core 16 basalt	13	0.115	0.058	0.20	3.5	0.15	0.16	3
Core 4 basalt	23	0.126	0.096	0.91	9.4	0.23	0.17	15
Core 19 breccia	33	0.138	0.12	0.37	3.1	0.21	0.28	6
Core 24 (2) breccia	32	0.163	0.41	0.89	2.2	0.61	0.63	7
Core 24 (1) breccia [a]	24	0.190	0.92	1.2	1.3	1.0	1.1	4
Core 8 (4) breccia	18	0.177	0.27	1.8	6.6	0.97	0.95	6
Core 8 (2) breccia	13	0.177	0.82	1.3	1.6	0.97	0.95	2
Core 8 (3) breccia	18	0.214	1.1	2.7	2.5	1.6	1.6	2
Core 8 (1) breccia	18	0.222	0.55	2.7	4.9	1.5	1.6	1
Core 7 (2) breccia	15	0.236	0.37	2.1	5.7	1.0	1.3	5
Core 7 (1) breccia	42	0.252	0.53	2.1	4.0	1.2	1.3	20
Core 36 breccia	23	0.248	2.0	3.0	1.5	2.4	2.4	6
Core 15 breccia	42	0.255	0.38	2.6	6.7	1.3	1.2	4
Core 20 breccia	18	0.271	2.3	4.6	2.0	3.3	3.2	3
UA-1, C87 breccia	4	0.29	–	–	–	5.4	–	–

[a] A 2-cm spacing was used for the Core 24 (1) sample.

summarized in Table 3. In most of the samples, the effect of scale, or the length required to achieve an approximately constant value is limited to less than 7 cm; and for 8 of the 14 samples, this length is less than 5 cm. This result is comparable to the observations on granites by others (Atkinson and Titchell, 1985; Skagius, 1986; Valkiainen et al., 1996). However, two samples, Core 4 and Core 7 #1, exhibited greater effects of scale in the formation factors, with the lengths of 15 cm and 20 cm, respectively, required to achieve an approximately constant value; though the appearance of this effect in Fig. 3 is somewhat deceptive due to the scaling employed in that figure. The Core 4 basalt sample contained an unweathered, axial fracture in the central portion of the sample that yielded higher formation factor values in that portion of the sample. The Core 7 #1 breccia sample contained a large, dense 7.5-cm clast containing phenocrysts and open vesicles, which likely contributed to the greater scale effect exhibited in this sample. The specific influence of this clast is difficult to ascertain; it is comprised of a low porosity matrix material that would inhibit the diffusive transport of molecules, however, preferential flow surrounding such clasts in the breccia samples is also suspected (Keller and Ibrahim, 1982; Benning, 2008).

4.2. The effects of spatial heterogeneities on diffusion

The resulting maximum, minimum, and average formation factors derived though electrical conductivity testing of adjacent 1 cm sections (2 cm sections for the 24-cm long Core 24 sample) are summarized for each sample tested in Table 3. The "factor" difference indicates the ratio of the maximum to minimum estimated formation factor from the adjacent subsections for each sample and indicates the proportional variability of the formation factor in each sample. While no formal uncertainty analyses were performed for the electrical conductivity methods, the estimated experimental errors are approximately 30% and are far less in magnitude than the differences between maximum and minimum estimated formation factors.

Each sample tested displayed some degree of spatial variability in the formation factors derived from adjacent sections of core; the degree of variability is generally greater though for the breccias that are characterized by obvious heterogeneities than for the more homogeneous breccia and basalt samples. To illustrate this result, two of the more extreme sample results are shown in Fig. 4, along with photographs and CT scans. The CT scans illustrate relative densities of the material. As an example, in the Core 7 breccia sample (Fig. 4a, b, c), the high and low formation factors are likely related to the relative proportions of high and low density material in the specific sample section. In contrast, the Core 19 sample appears, in the CT scans, to be comprised of clasts with relatively similar densities, and there is correspondingly less variability in the adjacent measured formation factors (Fig. 4d, e, f).

As summarized in Table 3, when multiple samples from the same lithologic layer were tested, there were often significant differences between the formation factors for that layer. For example, the Core 8 #1 and #3 samples displayed an average formation factor that was greater than that of the Core 8 #2 and #4 samples by a factor of approximately 1.6. Similarly, the Core 24 #1 sample had a formation factor that was a factor of 1.6 greater than that of the Core 24 #2 sample. These results indicated that there are potentially significant effects of spatial heterogeneities within lithologic layers.

Comparison of the results shown in Table 3 and Fig. 3 illustrates that there are significant effects of spatial heterogeneities with regards to various lithologic layers as well. As noted previously, the various lithologic layers present at the Cannikin test shot location display formation factors that vary by more than one order of magnitude, while the maximum and minimum formation factors found in all of the Amchitka Island samples tested in this study vary by more than two orders of magnitude (on the order of 10^{-4} for the andesite and 10^{-2} for the more porous of the breccia samples).

A comparison of the average and the asymptotic values of the formation factors derived by electrical conductivity testing

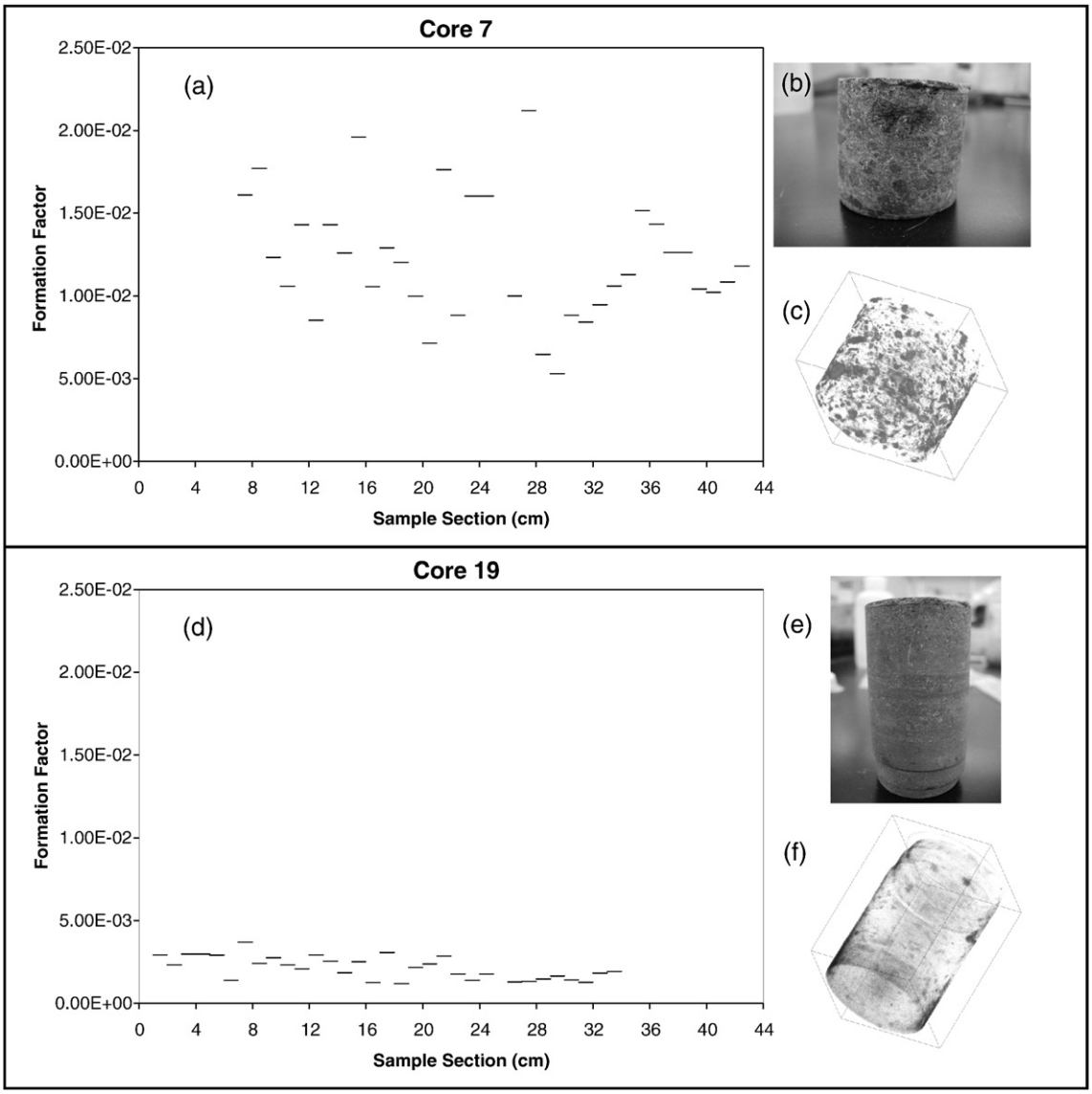

Fig. 4. Spatial variability of the measured formation factor across 1-cm thick adjacent sample sections for (a) Core 7 and (d) Core 19. Photographs of adjacent 51-mm diameter core samples for (b) Core 7 and (e) Core 19. 3-D view of samples produced by X-ray CT imaging, with dark colors represent high densities, 51 mm diameter samples of (c) Core 7 and (f) Core 19.

for each sample, as summarized in Table 3, indicates that for nearly all of the samples, except for the Core 4 and Core 19 samples, the two values are approximately equal. This observation is in agreement with the results of Löfgren and Neretnieks (2006) for granites. These results indicate that an adequate estimate for even the most heterogeneous of the breccia samples can be obtained either by conducting tests on multiple small samples or by conducting tests on longer samples, which allows for flexibility in the experimental design.

4.3. Formation factor/porosity relationships

Common practice is to derive an empirical relationship between the formation factor and the porosity of a porous medium, based on Archie's Law (Parkhomenko, 1967; Keller and Ibrahim, 1982). Reimus et al. (2007) determined an empirical relationship for the geometric factor (it is noted that the authors employ a definition of the "formation factor" that does not include the porosity, here it is referred to as the geometric factor) that is dependent on not only the porosity, but the permeability as well. The authors, however, noted that their empirically-derived relationship was developed specifically for saturated volcanic rocks from the Nevada Test Site and would not necessarily be the same for other types of rocks. The relationship between the logarithms of the average formation factors derived by the electrical conductivity methods and the porosities is illustrated in Fig. 5. The derived equation from this study is:

$$log(G_f) = 7.3759\phi - 2.8861 \quad (6)$$

For comparison, the relationship derived by Reimus et al. (2007) is also illustrated in Fig. 5. While the empirical

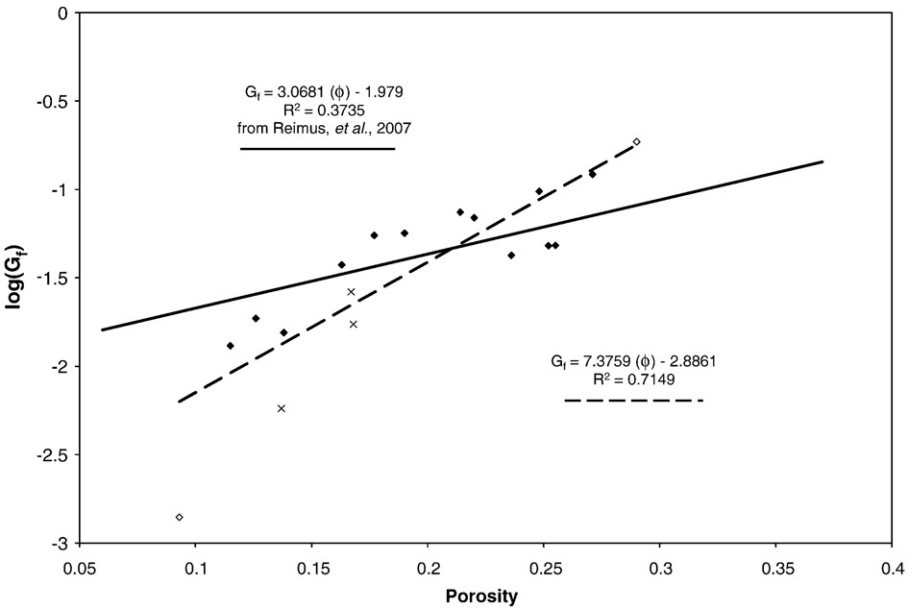

Fig. 5. Geometric factor as a function of porosity. The diamonds denote geometric factors measured by electrical conductivity and are included in the regression analysis, the open circles represent geometric factors measured by electrical conductivity in the preliminary investigations, and the xs represent geometric factors measured by tracer-based methods.

relationships illustrated in Fig. 5 are obviously not identical, it is not unlikely that they may fall within confidence intervals, which were not specified in either study. An important factor to consider is that breccias commonly contain clay minerals, and as noted by Keller and Ibrahim (1982), the conducting properties of clay minerals may result in difficulties in the application of Archie's Law.

Reimus et al. (2007) also derive an equation to estimate the formation factor from the porosity and permeability (K_i) data. The equation is given as:

$$\log G_f = (1.42 \pm 1.60) + (1.91 \pm 1.29)\phi + (0.19 \pm 0.089)(\log K_i) \quad (7)$$

In these studies, the permeability was measured on only two samples, one derived from Core 19 and one from Core 24. The permeabilities, measured in a fixed-wall type rock permeameter under a simulated overburden pressure of 1.38×10^4 kPa (2000 psi), were 2.17×10^{-14} m^2 and 3.30×10^{-13} m^2 for Core 19 and Core 24, respectively. The estimated logarithm of the formation factors from Eq. (7) for these two cores are compared to the experimentally determined values from both electrical methods and through-diffusion methods in Table 4. In all cases, the experimentally determined values are lower than the estimates provided by Eq. (7). One possible factor causing some of the discrepancy between these values may have been that the permeabilities in these studies were measured under pressure, while it does not appear that the permeability measurements used to derive Eq. (7) were conducted under pressures (Reimus et al., 2007), though there was only a 3–4% difference between porosities measured under the same simulated pressure and those measured under atmospheric pressure.

If the data illustrated in Fig. 4 is expressed in the manner of Archie's Law, the relationship becomes:

$$F_f = 1.20\phi^{3.05} \quad (8)$$

In comparison, the exponent in Eq. (8), which is referred to as the Archie's exponent m, is considerably higher than the values for m in published literature for various rock types (Parkhomenko, 1967). Wong et al. (1984) have shown that m is related to the "skewness of the pore-size distribution of the rock." This result would indicate that there is a widely varying distribution of pore sizes in the extrusive volcanic rocks from Amchitka Island, which is not unexpected considering the demonstrated heterogeneities, in particular, of the breccias.

Table 4
The value of log(G_f) derived from Eq. (7) and measured porosities and permeabilities (Reimus et al., 2007) compared to experimentally determined values derived from both electrical and tracer-based methods.

Method	log(G_f)	
	Core 19	Core 24
Eq. (7)	-1.03 ± 0.49	-0.60 ± 0.75
Electrical conductivity experiment	-2.7	-2.1 ± 0.1
Through-diffusion experiment	-3.1	-2.45 ± 0.05

4.4. Probability density functions of the formation factor

The results of each set of formation factors for the adjacent 1-cm subsamples for each sample derived from electrical conductivity testing, as presented in Fig. 4 (summary data found in Table 3), were statistically tested using either the Shapiro–Wilks W Test when there were less than 50 data points or the D'Agostino K-squared Test when there were greater than 50 data points (Gilbert, 1987) to ascertain the distribution (normal or lognormal) of the formation factor for each core sample. Additionally, when multiple samples from the same drill core section were tested (as with Core 7, Core 8, and Core 24), the combined data sets for each drill core section were

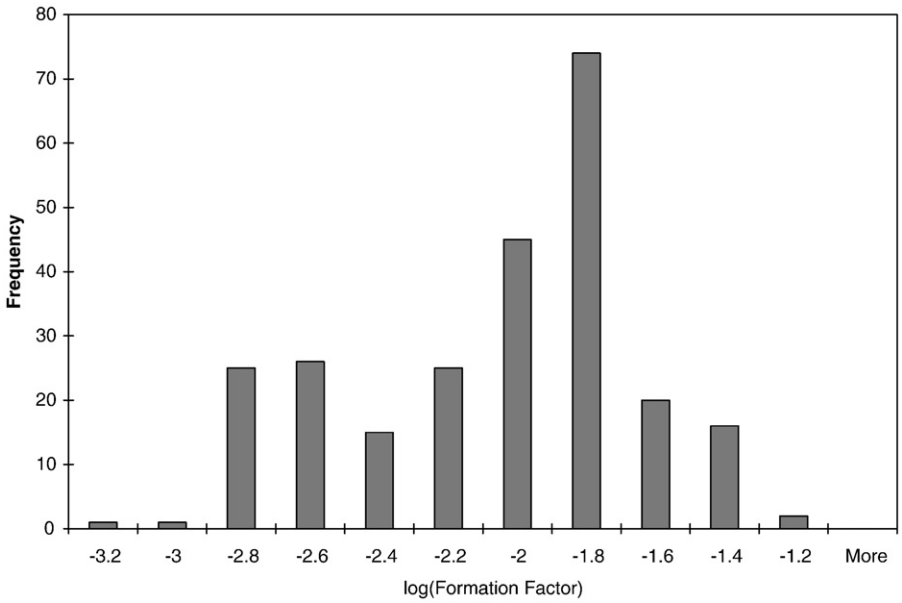

Fig. 6. Histogram of the natural logarithm of the formation factors measured in this study on all core samples at adjacent 1-cm sample sections using electrical methods.

analyzed. The distribution of the natural logarithm (base e) of the entire data set for all of the samples and layers, as presented in the histogram in Fig. 6, was also analyzed. The results of the statistical analyses of the PDFs are summarized in Table 5.

The results summarized in Table 5 indicate that for each core sample, as well as for the combined data sets of different samples from the same drill core section, the PDFs are all normal either at the $\alpha = 0.05$ or the $\alpha = 0.02$ significance level, except for the Core 4 sample. The Core 4 sample PDF, in contrast, fits a lognormal distribution; this result can be explained by the presence of a visible unweathered fracture in the axial direction in the sample. Others have established that the porosity of unconsolidated porous materials follows a normal distribution while the permeability follows a lognormal distribution (Freeze, 1975), and so for the rocks with a distribution of the formation factor that fits the normal distribution, it is likely that the distribution of the porosity plays a dominant role in the formation factor distribution, at least at the scale of these measurements. In contrast, in samples with relatively large-scale heterogeneities, such as the fracture in the Core 4 sample, the distribution may become lognormal as a result of the tendency for extreme values in the resulting data sets.

When all of the geologic layers sampled from the UAe-1 borehole are considered together, as in Fig. 6, because of the order of magnitude differences between the formation factors to the depth of the Cannikin test shot, the distribution of the subsurface as a whole in the Cannikin test shot vicinity can be described by a lognormal distribution. This finding is similar to

Table 5
Summary of statistical tests to describe PDF of the formation factor from the data for each sample.

Sample	Number of data points, n	PDF at $\alpha = 0.05$	PDF at $\alpha = 0.02$	Mean	Standard deviation
Core 4 basalt	23	Not lognormal	Lognormal	−6.23 [a]	0.56 [b]
Core 7 #1 breccia	36	Normal	Normal	1.21E−2	0.37E−2
Core 7 #2 breccia	15	Normal	Normal	1.16E−2	0.38E−2
Core 8 #1 breccia	17	Normal	Normal	1.49E−2	0.50E−2
Core 8 #2 breccia	13	Normal	Normal	9.70E−3	1.5E−3
Core 8 #3 breccia	16	Normal	Normal	1.59E−2	0.38E−2
Core 8 #4 breccia	15	Normal	Normal	9.72E−3	3.8E−3
Core 15 breccia	39	Normal	Normal	1.27E−2	0.48E−2
Core 16 basalt	12	Normal	Normal	1.46E−3	0.36E−3
Core 19 breccia	33	Normal	Normal	2.14E−3	0.68E−3
Core 20 breccia	18	Normal	Normal	3.28E−2	0.56E−2
Core 24 #1 breccia	12	Normal	Normal	1.07E−2	0.08E−2
Core 24 #2 breccia	32	Normal	Normal	6.10E−3	1.1E−3
Core 36 breccia	22	Normal	Normal	2.42E−2	0.29E−2
Core 7 all	51	Normal	Normal	1.20E−2	0.37E−2
Core 8 all	61	Normal	Normal	1.28E−2	0.47E−2
Core 24 all	44	Normal	Normal	7.36E−3	2.3E−3
All data	303	Not lognormal	Lognormal	−4.82 [a]	0.94 [b]

[a] The mean is given as the mean of $\ln(F_f)$ to characterize the lognormal distribution.
[b] The standard deviation is given as the standard deviation of $\ln(F_f)$ to characterize the lognormal distribution.

that of Löfgren (2007), who reported a lognormal distributions of the formation factor PDF in two boreholes at a site in Sweden. The result for this site is also in concurrence with the high *m*-factor in Archie's Law, which, as noted in Section 4.3, indicates a high-skewness in the formation factor data for the site. Some caution is noted however, because though the entire set statistically can be described by a lognormal distribution at the $\alpha = 0.02$ significance level, the lognormal distribution hypothesis is rejected at the $\alpha = 0.05$ significance level, indicating that the D'Agostino test statistic is borderline. This may be attributed to the sparseness of data with values around those of the Core 24 values.

4.5. Diffusion in the Amchitka Island subsurface

The results presented in the preceding are expected to enhance the understanding of the fate and transport of radionuclides at Amchitka Island, Alaska. Regarding the effects of scale on diffusion, as presented in Section 4.1, it does not appear that scale effects are a significant concern for estimating diffusivities at the island, at least at the scale of the laboratory measurement, up to 42 cm in length. While there are some effects of scale, these are mostly limited to diffusion lengths of approximately 6 cm. Overall, at the scale of the laboratory measurements, the pore networks for the basalts and breccias studied appear to be well-

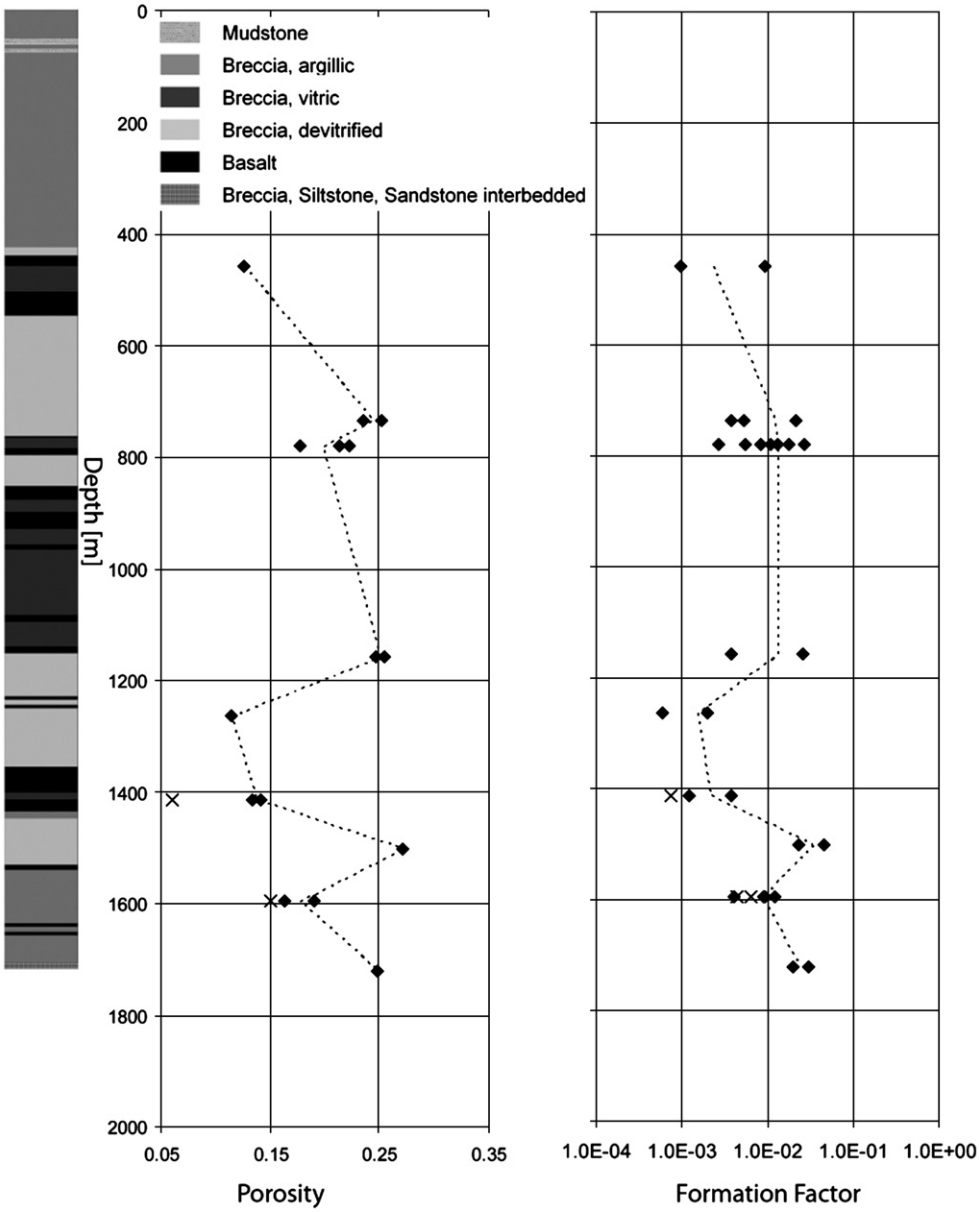

Fig. 7. The variation of the measured porosities and formation factors with depth of sample origin, compared to the UAe-1 (Cannikin vicinity) core log, displaying four basic categories of rock type: basalt, devitrified breccia, vitric breccia, and argillic breccia. The diamonds represent the porosities and the maximum and minimum formation factors measured by water saturation and electrical methods, respectively. The xs represent the effective porosities and formation factors measured by tracer methods. The dashed lines connect the average measurements for each core sample.

connected, in agreement with the results for the granites studied by Löfgren and Neretnieks (2006). There should, however, be some caution in studying samples that are too small such that pores become connected that would not be connected at larger scales and such that the influence of induced microcracks is too large, as was noted by Reimus et al. (2007). This effect was observed in these investigations in the through-diffusion experiments, though other than the potential effect on the measured porosity in the Core 19 sample, the impacts are generally small in comparison to the heterogeneities observed between geologic layers. In comparison of the results of these investigations to those of previous investigations into diffusion at Amchitka Island, however, the impact of using too small a sample are more pronounced.

The results of these investigations reveal, for the samples investigated, formation factors ranging from 1.3×10^{-4} to 5.4×10^{-2} for the island and from 7.4×10^{-4} to 3.3×10^{-2} for the Cannikin test shot location. For the basalts, the estimated formation factors are between 1.5×10^{-3} and 2.3×10^{-3}, which is much lower than the range estimated for basalts in Brown's (2000) study of 3.6×10^{-2} and 4.2×10^{-1}. These investigations indicate a much wider range of formation factors for the breccias at the island of between 7.4×10^{-4} to 5.4×10^{-2}, as compared to the range for breccias given by Brown of 1.6×10^{-2} to 7.5×10^{-2} (though it is noted that in Brown's investigations fewer breccia samples were analyzed). In comparing these results, some consideration should be given to the sample sizes used in Brown's study, which were much smaller than those used in these investigations. Therefore, it is likely that the use of small samples could allow pores to become connected that would otherwise not be connected in larger samples, significantly contributing to the overestimation of the formation factors for both the basalts and breccias in Brown's study.

The results shown in Fig. 7 illustrate the porosity and formation factor profile with depth at the Cannikin test shot location, to the approximate depth of the Cannikin detonation. The profile suggests a strongly layered subsurface with regards to the variability in both the formation factor, as discussed in the preceding, and the bulk porosity, which ranges from 11.5% to 27.1%. In a previous groundwater model for the island, Wheatcraft (1995) recommended that that model could be improved by the consideration of a layered geologic system. Later groundwater models by Hassan and Chapman (2006) and Wagner (2007) applied the effective porosity profile from magnetotelluric (MT) data illustrated in Fig. 8. The bulk porosity data appears to closely match the Archie's $m=2$ line for the MT profile; though because of the scale of measurements in the MT profile, the profile is smoothed as compared to the laboratory porosity measurements. Overall, the bulk porosities tend to be higher than those used in the groundwater models (Wagner, 2007); however, the estimate of the effective porosity derived from the Core 19 through-diffusion experiment is less than the $m=1.5$ value that was applied in the groundwater model at that location.

Wagner (2007) considered the influence of an andesite sill layer in the groundwater model for the Long Shot (LS) test site. This sill is characterized by an extensive fracture network that yields a high hydraulic conductivity for the layer. When the influence of this sill was considered, the estimated groundwater travel time (no diffusion or sorption was considered) to the ocean floor from the test cavity was reduced from an estimated 1400–4700 years to an estimated 400–1400 years, indicating the importance at that site of a layered approach to modeling. While LS-vicinity cores were not available for these investigations, the estimated matrix porosity and matrix formation factor for an andesite core sample derived from the Milrow vicinity are very low, at 9% and 1.3×10^{-4}, respectively, for the

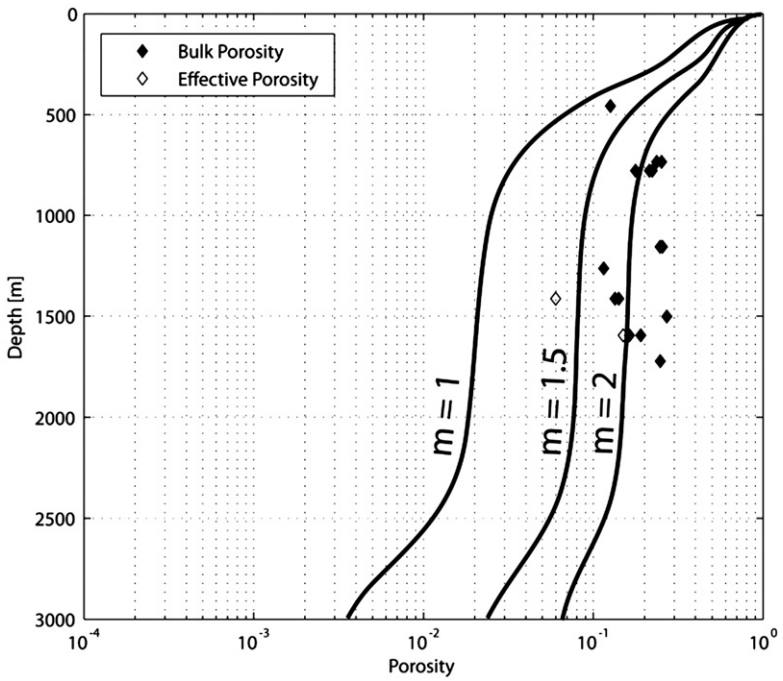

Fig. 8. Comparison of the depth profile of the porosities measured in these studies to the profile of the porosities derived in magnetotellurics studies (from Unsworth et al., 2007).

site. This suggests that there is a lower potential for diffusion and subsequent retardation of radionuclides in this layer as compared to other layers.

5. Conclusions

The investigations indicate that there is some effect of scale on measured intrinsic diffusion coefficients and formation factors, but these effects are generally small in comparison to variability between lithologic layers. These effects are also generally limited to approximately 6 cm for most samples and are well-correlated with observed heterogeneous features. Similar to the results of Löfgren and Neretnieks (2006) for granites, the pore structures of the breccias and basalts present in the subsurface at Amchitka Island appear to be well-connected at the scale of laboratory measurements (up to 42 cm in length). For most of the samples investigated, the average formation factor for adjacent 1-cm sections of rock is approximately equal to the asymptotic value of the formation factor for increasing sample lengths, thereby implying that an adequate estimate for even the most heterogeneous of the breccia samples can be obtained either by conducting tests on multiple small samples or by conducting tests on longer samples, which allows for flexibility in experimental design. An important conclusion resulting from this study is that there is a potential for the estimated formation factor to be misrepresented by an order of magnitude if multiple samples are not tested.

For individual geologic layers, the investigations indicate that the probability density function of the formation factor is normal, except when the sample is influenced by features with different properties than the surrounding matrix properties (e.g., an unconnected and unweathered fracture). However, the probability density function for the formation factor throughout the depth of the Cannikin vicinity subsurface shows a lognormal distribution, due to the order of magnitude differences between lithologic layers. The large skewness of the distribution is corroborated by the high *m*-factor in Archie's Law for the relationship between the porosity and formation factor for the Amchitka Island samples. An understanding of the probability density function is essential to stochastic modeling efforts.

The intrinsic diffusion coefficients and formation factors derived in these studies are much lower than those derived in previous, more limited diffusion studies for Amchitka Island. The formation factor and porosity profiles for the Cannikin test site show a strongly layered subsurface with a large spatial variability found in both parameters. The results of these investigations are anticipated to reduce some of the uncertainties associated with the radionuclide transport modeling at the island.

Acknowledgments

The authors would like to thank the Inland Northwest Research Alliance Subsurface Science Program, the Consortium of Risk Evaluation with Stakeholder Participation II through the Department of Energy cooperative agreement (award no. DE-FG26-00NT40938 and DE-FC01-06EW07053), and the Water and Environmental Research Center of the University of Alaska Fairbanks for funding this project. The results and conclusions expressed here reflect the opinions of the authors and do not necessarily represent the views of the funding agencies. Thanks are due to Dr. Richard Wies of the University of Alaska Fairbanks for assistance with electrical conductivity testing and to Walter Fourie of the University of Alaska Fairbanks for the preparation of figures. We sincerely thank the anonymous reviewers for their efforts and suggestions.

References

Altman, S.J., Uchida, M., Tidwell, V.C., Boney, C.M., Chambers, B.P., 2004. Use of X-ray absorption imaging to examine heterogeneous diffusion in fractured crystalline rocks. Journal of Contaminant Hydrology 69, 1–26.

Appelo, C.A.J., Wersin, P., 2007. Multicomponent diffusion modeling in clay systems with application to the diffusion of tritium, iodide, and sodium in Opalinus Clay. Environmental Science and Technology 41, 5002–5007.

Atkinson, A., Titchell, I., 1985. Diffusive transport in granite studied using ionic conductivity. United Kingdom Atomic Energy Authority, Harwell Report, AERE R 1127.

Bear, J., 1972. Dynamics of Fluids in Porous Media. Dover Publications, Inc., New York.

Benning, J.L., 2008, The effects of scale and spatial heterogeneities on diffusion in volcanic breccias and basalts: Amchitka Island, Alaska, Ph.D. Dissertation, Department of Civil and Environmental Engineering, University of Alaska Fairbanks.

Benning, J.L., Barnes, D.L., Burger, J., Kelley, J.J., 2009. Amchitka Island, Alaska: moving towards long-term stewardship. Polar Record 45, 133–146.

Brace, W.F., Orange, A.S., Madden, T.R., 1965. The effect of pressure on the electrical resistivity of water-saturated crystalline rocks. Journal of Geophysical Research 70 (22), 5669–5678.

Bradbury, M.H., Green, A., 1985. Measurement of important parameters determining aqueous phase diffusion rates through crystalline rock matrices. Journal of Hydrology 82, 39–55.

Brown, N., 2000, Modeling the diffusion of reactive and nonreactive solutes in cores from the Cannikin test site, Amchitka Island, Alaska, M.S. Thesis, Water Resources Management, University of Nevada, Las Vegas.

Claassen, H.C., 1978. Hydrologic processes and radionuclide distribution in a cavity and chimney produced by the Cannikin nuclear explosion, Amchitka Island, Alaska. U.S. Geological Survey professional paper 712-D, Washington, D.C.

Crank, J., 1975. The Mathematics of Diffusion, Second Edition. Oxford University Press, Inc., New York.

CRC Press, 2008. Handbook of Chemistry and Physics, 88th Edition. CRC Press, New York.

Cussler, E.L., 1984. Diffusion: Mass Transfer in Porous Media. Cambridge University Press, New York.

Daniel, V., Albright, J.G., 1991. Measurement of mutual-diffusion coefficients for the system KNO_3–H_2O at 25 °C. Journal of Solution Chemistry 20 (6), 633–642.

Fetter, C.W., 1994. Applied Hydrogeology. Macmillan College Publishing Company, New York.

Freeze, R.A., 1975. A stochastic-conceptual analysis of one-dimensional groundwater flow in nonuniform homogeneous media. Water Resources Research 11 (5), 725–741.

Gard, L.M., Lee, W.H., Way, R.J., 1969a. Preliminary lithologic log of drill hole UAe-1 from 0 to 5,028 feet, Amchitka Island, Alaska. United States Department of the Interior Geological Survey, Federal Center, Denver, Colorado, USGS-474-46.

Gard, L.M., Lee, W.H., Way, R.J., 1969b. Preliminary lithologic log of drill hole UAe-1 from 5,000 to 7,000 feet, Amchitka Island, Alaska. United States Department of the Interior Geological Survey, Federal Center, Denver, Colorado, USGS-474-47.

Gelhar, L.W., Welty, C., Rehfeldt, K.R., 1992. A critical review of data on field-scale dispersion in aquifers. Water Resources Research 28 (7), 1955–1974.

Gilbert, R.O., 1987. Statistical Methods for Environmental Pollution Monitoring. Van Nostrand Reinhold, New York.

Hassan, A., Pohlmann, K., Chapman, J., 2002. Modeling groundwater flow and transport of radionuclides at Amchitka Island's underground nuclear tests: Milrow, Long Shot, and Cannikin. Desert Research Institute, Division of Hydrologic Sciences, Nevada, Publication No. 45172.

Hassan, A., Chapman, J., 2006. Verification and uncertainty reduction of Amchitka underground nuclear testing models. Desert Research Institute, DOE/NV/13609-46.

Heath, M., Montoto, M., Rodriguez Rey, A., Ruiz de Argandona, V., Menendez, B., 1992. Rock matrix diffusion as a mechanism of radionuclide retardation: a natural analogue study of El Berrocal granite, Spain. Radiochimica Acta 58/59, 379–384.

Keller, G.V., Ibrahim, A.W., 1982, Research on the physical properties of geothermal reservoir rocks, Prepared for the US Department of Energy, Report DOE/ET/28366-5, Argonne, Illinois, Prepared by The Department of Geophysics, Colorado School of Mines, Golden, Colorado.

Klinkenberg, L.J., 1951. Analogy between diffusion and electrical conductivity in porous rocks. Bulletin of the Geological Society of America 62, 559–564.
Krishna, R., Wesselingh, J.A., 1997. The Maxwell-Stefan approach to mass transfer. Chemical Engineering Science 52 (6), 861–911.
Lever, D.A., Bradbury, M.H., Hemingway, S.J., 1985. The effect of dead-end porosity on matrix diffusion. Journal of Hydrology 80, 45–76.
Lin, C., Pirie, G., Trimmer, D.A., 1986. Low permeability rocks: laboratory measurements and three-dimensional microstructural analysis. Journal of Geophysical Research 91 (B2), 2173–2181.
Löfgren, M., 2007. Formation factor logging by electrical methods in KFM01D and KFM08C, Forsmark site investigations. Swedish Nuclear Fuel and Waste Management Co., SKB, Site investigation report P-07-138, Stockholm, Sweden.
Löfgren, M., Neretnieks, I., 2002. Formation factor logging by electrical methods: background and methodology. Swedish Nuclear Fuel and Waste Management Co., SKB, Technical report TR 02-27, Stockholm, Sweden.
Löfgren, M., Neretnieks, I., 2006. Through-electromigration: a new method of investigating pore connectivity and obtaining formation factors. Journal of Contaminant Hydrology 87, 237–252.
Mayr, S.I., Burkhardt, H., Popov, Y., 2007. Estimation of hydraulic permeability considering the micro morphology of rocks of the borehole YAXCOPOIL-1 (impact crater Chicxulub, Mexico). International Journal of Earth Sciences Review Article, July 2007.
Merritt, M.L., Fuller, R.G. (Eds.), 1977. The Environment of Amchitka Island, Alaska, Technical Information Center, Energy Research and Development Administration, NVO-79, Washington, D.C.
Moridis, G.J., 1998. A set of semianalytical solutions for parameter estimation in diffusion cell experiments. Report LBNL-41857, Lawrence Berkeley Nations Laboratory, Berkeley, California.
Moridis, G.J., 1999. Semianalytical solutions for parameter estimation in diffusion cell experiments. Water Resources Research 35 (6), 1729–1740.
Neretnieks, Ivars, 1980. Diffusion in the rock matrix: an important factor in radionuclide retardation? Journal of Geophysical Research 85 (B8), 4379–4397.
Neretnieks, Ivars, 1993. Solute Transport in Fractured Rock — Applications to Radionuclide Waste Repositories, Flow and Contaminant Transport in Fractured Rock. Academic Press.
Ohlsson, Y., 2000, Studied of ionic diffusion in crystalline rock, Doctoral thesis at the Royall Institute of Technology, Stockholm, Sweden.
Parkhomenko, E.I., 1967. Electrical Properties of Rocks. Plenum Press, New York.
Pletnikoff, K., 2008. Amchitka watch program. 11–15 February 2008. Anchorage, Alaska: Alaska Forum on the Environment.
Raghupatruni, S.R., 2004. Measurement of Effective Diffusion on Andesite Rock, Amchitka Island, Alaska, M.S. Thesis, University of Alaska Fairbanks.
Reimus, P.W., Callahan, T.J., Ware, S.D., Haga, M.J., Counce, D.A., 2007. Matrix diffusion coefficients in volcanic rocks at the Nevada test site: influence of matrix porosity, matrix permeability, and fracture coating minerals. Journal of Contaminant Hydrology 93, 85–95.
Schild, M., Siegesmund, S., Vollbrecht, A., Mazurek, M., 2001. Characterization of granite matrix porosity and pore-space geometry by in situ and laboratory methods. Geophysical Journal International 146, 111–125.
Siitari-Kauppi, M., Lindberg, A., Hellmuth, K., Timonen, J., Väätäinen, K., Hartikainen, J., Hartikainen, K., 1997. The effect of microscale pore structure on matrix diffusion — a site-specific study on tonalite. Journal of Contaminant Hydrology 26, 147–158.
Skagius, K., 1986, Diffusion of dissolved species in the matrix of some Swedish crystalline rocks, Ph.D. Thesis, Department of Chemical Engineering, Royal Institute of Technology, Sweden.
Skagius, K., Neretnieks, I., 1986a. Porosities and diffusivities of some nonsorbing species in crystalline rocks. Water Resources Research 22 (3), 389–398.
Skagius, K., Neretnieks, I., 1986b. Diffusivity measurements and electrical resistivity measurements in rock samples under mechanical stress. Water Resources Research 22 (4), 570–580.
Snyder, K.A., 2001. The relationship between the formation factor and the diffusion coefficient of porous materials saturated with concentrated electrolytes: theoretical and experimental considerations. Concrete Science and Engineering 3, 216–224.
Snyder, K.A., 2003. Condition assessment of concrete nuclear structures considered for entombment. U.S. Nuclear Regulatory Commission, U.S. Department of Commerce, National Institute of Standards and Technology, NISTIR 7026.
Stokes, R.H., Woolf, L.A., Mills, R., 1957. Tracer diffusion of iodide ion in aqueous alkali chloride solutions at 25°. Journal of Physical Chemistry 61 (2), 1634–1636.
Telford, W.M., Geldart, L.P., Sheriff, R.E., 1990. Applied Geophysics, 2nd edition. Cambridge University Press, New York.
Tidwell, V.C., Meigs, L.C., Christian-Frear, T., Boney, C.M., 2000. Effects of spatially heterogeneous porosity on matrix diffusion as investigated by X-ray absorption imaging. Journal of Contaminant Hydrology 42, 285–302.
Towle, G.H., 1962. An analysis of the formation resistivity factor–porosity relationship of some assumed pore geometrics, SPWLA Transactions. Third Annual Well Logging Symposium.
Treybal, R.E., 1980. Mass Transfer Operations, 3rd edition. McGraw Hill Book Company, New York.
Unsworth, M., Soyer, W., Tuncer, V., Wagner, A., Barnes, D., 2007. Case history, hydrogeologic assessment of the Amchitka Island nuclear test site (Alaska) with magnetotellurics. Geophysics 72 (3), B47–B57.
U.S. Atomic Energy Commission (USAEC), 1972. Project Cannikin, D+30 day report, preliminary operational and test results summary, United states Atomic Energy Commission, Nevada operations Office, NVO-108, Las Vegas, Nevada.
U.S. Congress, Office of Technology Assessment, 1989. The Containment of Underground Nuclear Explosions, U.S. Government Printing Office, OTA-ISC-414, Washington, D.C.
Valkiainen, M., Aalto, H., Lehikoinen, J., Uusheimo, K., 1996. The effect of thickness in the through-diffusion experiment. Final Report, VTT Research Notes, vol. 1788. Technical Research Center of Finland.
Van Brakel, J., Heertjes, P.M., 1974. Analysis of diffusion in macroporous media in terms of a porosity, a tortuosity, and a constrictivity factor. International Journal of Heat and Mass Transfer 17, 1093–1103.
Wagner, A.M. 2007, Using geophysical constraints to determine groundwater travel times, seafloor arrival locations, and saltwater concentrations for transition zone depths at underground nuclear detonations on Amchitka Island, Ph.D. Dissertation, University of Alaska Fairbanks.
Walter, G.R., 1982. Theoretical an experimental determination of matrix diffusion and related solute transport properties o fractured tuffs from the Nevada Test Site. LA-9471-MS, Los Alamos National Laboratory, Los Alamos, NM.
Wheatcraft, S.W., 1995. Sea water intrusion model of Amchitka Island, Alaska. Nevada Operations Office, U.S. Department of Energy, DOE/NV/10845-59.
Wong, P., Koplik, J., Tomanic, J.P., 1984. Conductivity and permeability of rocks. Physical Review B 30 (11), 6606–6614.
Yamaguchi, T., Nakayama, S., 1998. Diffusivity of U, Pu and Am carbonate complexes in a granite from Inada, Ibaraki, Japan studied by through diffusion. Journal of Contaminant Hydrology 35, 55–65.

Glossary

δ:	Constrictivity factor of the pore structure, dmnl.
κ_R:	Conductivity of the saturated rock, $(\Omega\ \mathrm{m})^{-1}$
κ_S:	Conductivity of the solution, $(\Omega\ \mathrm{m})^{-1}$
τ:	Tortuosity of the pore structure, dmnl.
ϕ_e:	Effective porosity of a medium, dmnl.
A:	Cross-sectional area of a sample, m^2.
C_p:	Concentration in the pore water, mg/L.
D_i:	Intrinsic diffusion coefficient, m^2/s.
D_m:	Molecular, or free water, diffusion coefficient, m^2/s.
D_p:	Pore water diffusion coefficient, m^2/s.
F:	Faraday's constant, C/mol
F_f:	Formation factor of a porous medium, dmnl.
G_f:	Geometric factor of a porous medium, dmnl.
I:	Current, A.
L:	Length of the sample, m.
R:	Gas constant, J/mol K
T:	Temperature, K
ΔU:	Potential drop, V
z:	ion charge, dmnl.